

High-speed infrared photonic band microscope using hyperspectral Fourier image spectroscopy

TOMOHIRO AMEMIYA,^{1,*} SHO OKADA,² HIBIKI KAGAMI,² NOBUHIKO NISHIYAMA,^{1,2} YUANZHAO YAO,³ KAZUAKI SAKODA,³  AND XIAO HU⁴

¹Institute of Innovative Research (IIR), Tokyo Institute of Technology, Tokyo 152-8552, Japan

²Department of Electrical and Electronic Engineering, Tokyo Institute of Technology, Tokyo 152-8552, Japan

³National Institute for Materials Science, Tsukuba 305-0044, Japan

⁴International Center for Materials Nanoarchitectonics (WPI-MANA), National Institute for Materials Science, Tsukuba 305-0044, Japan

*Corresponding author: amemiya.t.ab@m.titech.ac.jp

Received 3 February 2022; revised 16 March 2022; accepted 17 March 2022; posted 17 March 2022; published 3 May 2022

In this study, we developed a photonic band microscope based on hyperspectral Fourier image spectroscopy. The developed device constructs an infrared photonic band structure from Fourier images for various wavelength obtained by hyperspectral imaging, which make it possible to speedily measure the dispersion characteristics of photonic nanostructures. By applying the developed device to typical photonic crystals and topological photonic crystals, we succeeded in obtaining band structures in good agreement with the theoretical prediction calculated by the finite element method. This device facilitates the evaluation of physical properties in various photonic nanostructures, and is expected to further promote related fields.

2022 Optica Publishing Group under the terms of the [Optica Open Access Publishing Agreement](#)

<https://doi.org/10.1364/OL.454865>

A photonic structure refers to a fine structure of dielectric permittivity and/or magnetic permeability with a typical length of the order of the wavelength of light. The interaction between light and matter in such structures can be used to conduct various light operations. Photonic structures, including photonic crystals, metamaterials, and topological photonic crystals, have been realized through the micromachining of semiconductors using nanoprocessing technologies [1–5]. These can be used to realize various optical phenomena that cannot normally be seen, such as confining light beyond the diffraction limit [6–8], slow light effects [9–11], optical trapping [12,13], and unidirectional propagation depending on the optical spin [14–16].

The photonic band determines the optical characteristics of photonic structures. It summarizes the dispersion relationships of the propagation modes within a target structure and is used when designing devices using the target structure. Conventionally, the photonic band is measured by evaluating the transmission/reflection characteristics of various photonic structures while changing the incident angle or polarization state [17]. However, this requires assembling an optical system whose form is suited to the sample state of each case, and considerable

time is required for measurements and evaluations, including the adjustment of the optical system.

To overcome these issues, a Fourier-image-spectroscopy-based method has been proposed. Fourier image spectroscopy is a type of wide-angle energy momentum spectroscopy [18,19]. It has mainly been investigated in the visible region owing to problems with sensitivity and resolution [20]. However, various photonic structures, such as topological photonic crystals and metamaterials, are heavily applied in the near-infrared band (800–1700 nm) [21–26]; therefore, band information in this range is strongly desired. In this regard, in 2017, a research group at Bristol University successfully observed the wide-range band structure in three dimensions in the near-infrared band using Fourier image spectroscopy [27]. They achieved improved sensitivity by constructing an optical-fiber-based spectroscopic system on a variable stage for acquiring Fourier images from a device; however, this system has not shown sufficient performance for practical use from the viewpoint of resolution and measurement time.

To solve these problems, in the present study, we developed a photonic band microscope based on hyperspectral Fourier image spectroscopy that is ready for practical use. Specifically, we successfully obtained a photonic band by using hyperspectral imaging on the imaging side along with high-speed/wide-angle energy momentum spectroscopy. We used this device to observe the band structure of actual Si-based photonic crystals and topological photonic crystals; the results were almost identical to those calculated using the finite element method with COMSOL software.

Figure 1 shows the configuration of the developed device. Firstly, we obtained collimated light from a fiber-output wide-band white light source (Bentham Ltd, WLS100, wavelength range: 300–2500 nm) through a lens (L_0) (4× Olympus Plan Achromat Objective, 0.10 NA). Light was then irradiated on the sample by an objective lens (L_1) (60× Olympus Plan Fluorite Objective, 0.9 NA) through a polarizer and a quarter-wave plate (these are inserted when it is necessary to change the state of polarization of incident light). The scattered light from the sample was observed using an imaging element through the 4f optical system consisting of two achromatic lenses (L_2 and L_3) ($f = 300$ mm). A dichroic mirror was inserted in the middle of

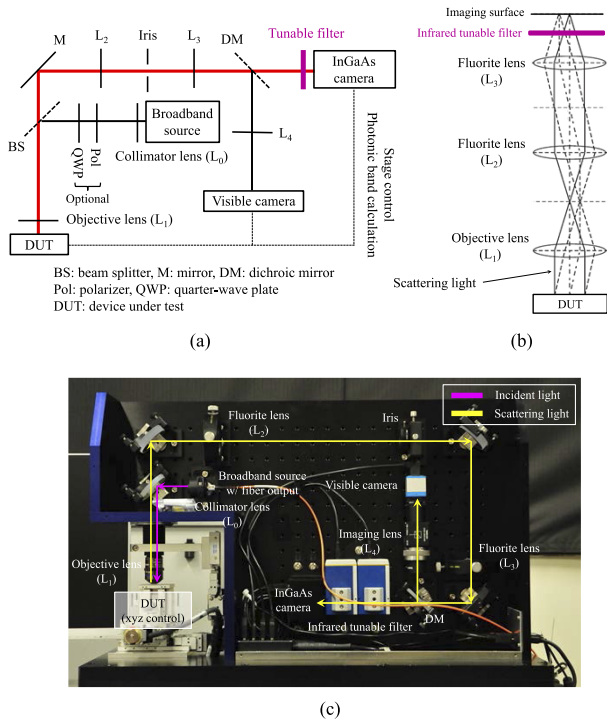


Fig. 1. (a) Configuration of the infrared photonic band microscope using Fourier image spectroscopy. (b) Light trajectory at bold line in Fig. 1(a). (c) Developed photonic band microscope.

the 4f optical system path, and the visible wavelength component of the broad-range white light source was used to observe the real image of the sample. This enabled the measurement of the band structure while confirming the local area of the photonic structure to be measured. In addition, a variable wavelength filter (VariSpec LNIR, bandwidth: 6 nm) was placed in front of the infrared camera (ARTCAM-008TNIR, pixel size: 30 μm × 30 μm) so that diffraction patterns of arbitrary wavelengths in the range of 850–1800 nm could be obtained. Further, the device had dimensions of only 320 (W) × 520 (H) × 700 (D) [mm].

Figure 2(a) shows the algorithm for obtaining a photonic band structure by using the above-described configuration. Given the aim of achieving high speed and versatility, we set up the following series of operations so that they can be performed fully automatically on the software. Firstly, the stage was moved to an arbitrary point in the target sample (spot size: 50 μm × 50 μm). Then, the Fourier image of the scattered light was observed using an infrared camera. Here, 3D Brillouin zone information could be obtained by observing the Fourier image while automatically subtracting the stage height, as shown in Fig. 2(b). Intensity information along the specified path was measured in the obtained Brillouin zone and then plotted as a specific wavelength (energy) intensity distribution in the reciprocal lattice space. This operation was performed for all wavelengths (energies) while changing the center wavelength of the tunable filter to reconstruct the photonic band structure. In this configuration, the resolution in the 2D and 3D directions of the Brillouin zone was rate-limited by the resolution of the infrared camera (pixel size: 30 μm × 30 μm) and the minimum movement distance of the stage (250 nm). In addition, the range of the Brillouin zone in each direction was determined by the effective angle of the objective lens (NA = 0.9 and θ = 64.1° in this study).

Table 1. Performance of the Photonic Band Microscope for 2D and 3D Measurements

	2D Normal	3D Precise ^a
Set wavelength range	from 0 to U (1260–1675 nm)	infrared full (850–1800 nm)
Set wavelength resolution	~5 nm	~3 nm
Set z-axis resolution	-	~300 nm (6 slices)
Brillouin zone area	2D (Γ-K-M)	3D (X-W-K-L-U)
Measurement time	~4.5 min	~100 min

^aOn the condition that the period of the photonic nanostructures in the 3D direction is of the same order as that in the 2D direction.

This device uses infrared hyperspectral imaging to obtain the infrared Fourier image for each wavelength, from which the band structure is directly reconstructed; this enables it to perform extremely rapid and versatile measurements. Table 1 shows the standard measurement time when a band structure is obtained using this device. Measurements can be performed for an infrared band with a wavelength of 850–1800 nm, that is, for band structures in the 2D direction (e.g., Γ-K-M) in an extremely short period of time (around 4–5 min). The band structures of several photonic structures were evaluated using this device.

Firstly, we show the results for a typical photonic crystal. Figure 3(a) shows a scanning electron microscope image of the element used in the evaluation. In this element, a square lattice photonic crystal was formed on a silicon on insulator (SOI) wafer (Si film thickness: 220 nm) having a lattice spacing of 580 nm and diameter/depth of circular holes of 180 nm/70 nm. Figure 3(b) shows a Fourier image of the scattered light from samples at each wavelength. There were clear changes due to the photonic band at each wavelength. Figure 3(c) shows the results of reconstructing the band structure by measuring the intensity along the Γ-X-M path corresponding to the square lattice in Fig. 3(b). Here, the X-point and M-point in Fig. 3(c) are actually ~3X/5 and ~3M/5 because the range of the experimental Brillouin zone in each direction is limited by the effective angle of the objective lens (NA = 0.9 and θ = 64.1°). In addition, the background for the SOI wafer is also shown in Fig. 3(d). Only the shading due to multiple resonances of the SOI wafer was observed in the background of the SOI wafer; further, a structure-derived photonic band was clearly observed for the SOI wafer on which the photonic crystal was formed. Figure 3(e) is a band structure analyzed by the finite element method (here, the box corresponds to the white box of Fig. 3(c)). For easy comparison, numbers are assigned to the corresponding parts between the experimental results and the analysis results. The areas surrounded by gray circles are regions where the band cannot be observed because the intensity of scattered light is quite weak, or the band cannot be seen due to the influence of the multiple resonance of the SOI wafer. The experimental and theoretical results were in good agreement, except that some points were shifted to the longer wavelength side (this is due to variations in the etching depth and sidewall roughness during fabrication), and this structure was characterized by the accidental degeneracy of the E mode and B1 mode near a wavelength of 1325 nm, as indicated in Fig. 3(e).

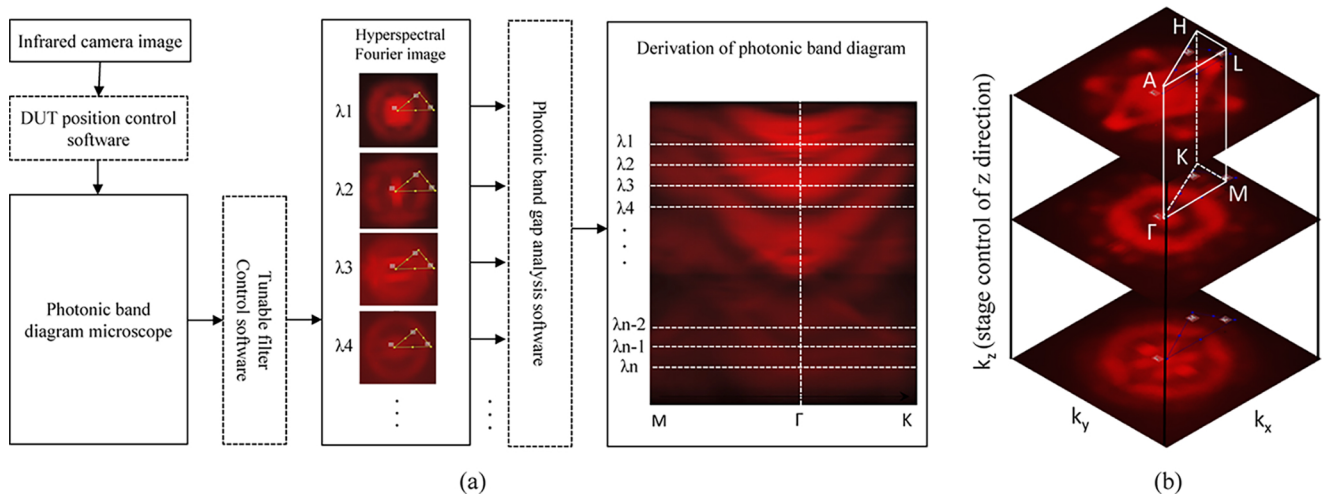


Fig. 2. (a) Algorithm for obtaining a photonic band structure. (b) 3D Brillouin zone information as a function of light energy obtained by observing the Fourier image. The series of operations were performed fully automatically on the software (Visualization 1).

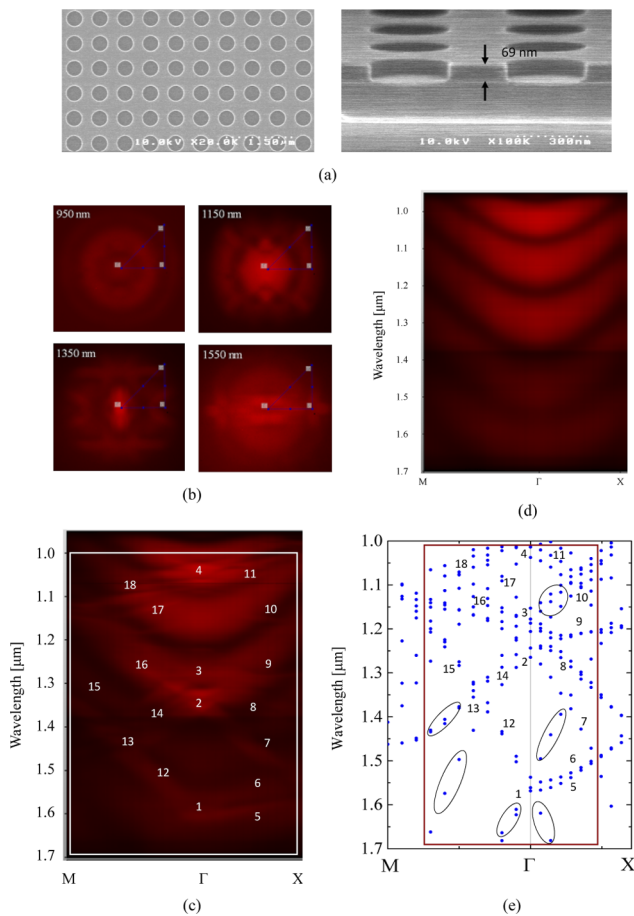


Fig. 3. (a) Scanning electron microscope image of a typical photonic crystal used in the evaluation. (b) Fourier image of the scattered light from samples at a certain wavelength. (c), (d) Reconstructed photonic band structures derived by measuring the intensity along the Γ -K-M path in Fourier images [(c) SOI wafer w/ photonic crystals; (d) SOI wafer w/o photonic crystals]. (e) Calculated photonic band structures based on the plane wave expansion method.

Next, we used this device to evaluate the topological photonic system, an area that has seen significant development in recent years. A characteristic of such a system is that photonic crystals different in topology can be realized by simultaneously controlling the interactions within and between cells. Using this characteristic enables the handling of optical information caused by topology, such as circularly polarized light (i.e., spin of light) and optical vortices (i.e., orbital angular momentum of light) [14,15,28,29,30].

Figure 4(a) shows a scanning electron microscope image of the element used for evaluation. In this study, we adopted a structure in which nanoholes are arranged in a deformed honeycomb lattice having C_{6v} symmetry on a SOI wafer (Si film thickness) as a photonic structure with Z2 topology. The period of the honeycomb structure was fixed at 800 nm, and the topology of the photonic structure was controlled by changing the distance R from the center of the hexagonal unit cell to the center of the nanohole and length L of one side of the nanohole [14,23].

Figure 4(b) shows the Fourier image of the scattered light from the sample at each wavelength. Here, we show the measurement results for two samples different in topology ($(R, L) = (230 \text{ nm}, 230 \text{ nm}), (290 \text{ nm}, 230 \text{ nm})$). Changes due to the photonic band can be seen at each wavelength; clear changes were also seen in the two structures different in topology. Figures 4(c) and 4(d) show the results of reconstructing the band structure by measuring the intensity along the Γ -K-M path corresponding to the honeycomb lattice in Fig. 4(b) (Figs. 4(c) and 4(d) show band structures of topological photonic structures for $(R, L) = (230 \text{ nm}, 230 \text{ nm})$ and $(R, L) = (290 \text{ nm}, 230 \text{ nm})$, respectively). Each band structure has a bandgap near 1.5 μm , which is the optical communication wavelength band, and the intensities of the upper and lower bands near the Γ point were reversed. It has been theoretically predicted and experimentally shown in two typical topological photonic systems different in topology that the electromagnetic modes of the p and d waves cause band inversion near the Γ point [14,15]. The reflection intensity of the d wave in the electromagnetic mode tended to be weaker than that of the p wave in experiments; therefore, we can conclude that our experimental results were in agreement with the theoretical predictions.

In conclusion, we have developed the infrared photonic band microscope based on hyperspectral Fourier image spectroscopy, which makes it possible to speedily measure the dispersion characteristics of photonic nanostructures. This device facilitates the evaluation of physical properties in various photonic nanostructures such as those in topological cavity surface emitting laser (TCSEL) [31], and is expected to further promote related fields.

Funding. Core Research for Evolutional Science and Technology, Japan Science and Technology Agency (JPMJCR18T4); Ministry of Internal Affairs and Communications (182103111); Japan Society for the Promotion of Science (19H02193, 21J14822).

Disclosures. The authors declare no conflicts of interest.

Data availability. Data underlying the results presented in this paper are not publicly available at this time but may be obtained from the authors upon reasonable request.

REFERENCES

1. N. Yu and F. Capasso, *Nat. Mater.* **13**, 139 (2014).

2. L. Lu, J. D. Joannopoulos, and M. Soljačić, *Nat. Photonics* **8**, 821 (2014).
3. A. B. Khanikaev and G. Shvets, *Nat. Photonics* **11**, 763 (2017).
4. B.-Y. Xie, H.-F. Wang, X.-Y. Zhu, M.-H. Lu, Z. D. Wang, and Y.-F. Chen, *Opt. Express* **26**, 24531 (2018).
5. S. Barik, A. Karasahin, C. Flower, T. Cai, H. Miyake, W. DeGottardi, M. Hafezi, and E. Waks, *Science* **359**, 666 (2018).
6. Z. Jacob, L. V. Alekseyev, and E. Narimanov, *Nat. Mater.* **7**, 435 (2008).
7. Z. Jacob, L. V. Alekseyev, and E. Narimanov, *Nat. Photonics* **4**, 648 (2010).
8. Y. A. Vlasov, M. O'Boyle, H. F. Hamann, and S. J. McNab, *Nature* **438**, 65 (2005).
9. T. Baba, *Nat. Photonics* **2**, 465 (2008).
10. T. Amemiya, S. Yamasaki, M. Tanaka, H. Kagami, K. Masuda, N. Nishiyama, and S. Arai, *Opt. Express* **27**, 15007 (2019).
11. K. L. Tsakmakidis, A. D. Boardman, and O. Hess, *Nature* **450**, 397 (2007).
12. H. Hu, D. Ji, X. Zeng, K. Liu, and Q. Gan, *Sci. Rep.* **3**, 1249 (2013).
13. E. Ottea and C. Denz, *Appl. Phys. Rev.* **7**, 041308 (2020).
14. L.-H. Wu and X. Hu, *Phys. Rev. Lett.* **114**, 223901 (2015).
15. Y. Yang, Y.-F. Xu, T. Xu, H.-X. Wang, J.-H. Jiang, X. Hu, and Z.-H. Hang, *Phys. Rev. Lett.* **120**, 217401 (2018).
16. N. Parappurath, F. Alpeggiani, L. Kuipers, and E. Verhagen, *Sci. Adv.* **6**, 6 (2020).
17. W. M. Robertson, G. Arjavalingam, R. D. Meade, K. D. Brommer, A. M. Rappe, and J. D. Joannopoulos, *Phys. Rev. Lett.* **68**, 2023 (1992).
18. I. Sersic, C. Tuambilangana, and A. F. Koenderink, *New J. Phys.* **13**, 083019 (2011).
19. J. F. Galisteo-López, M. López-García, A. Blanco, and C. López, *Langmuir* **28**, 9174 (2012).
20. R. Wagner and F. Cichos, *Phys. Rev. B* **87**, 165438 (2013).
21. Y. Wu, C. Li, X. Hu, Y. Ao, Y. Zhao, and Q. Gong, *Adv. Opt. Mater.* **5**, 1700357 (2017).
22. T. Amemiya, T. Kanazawa, S. Yamasaki, and S. Arai, *Materials* **10**, 1037 (2017).
23. H. Kagami, T. Amemiya, S. Okada, N. Nishiyama, and X. Hu, *Opt. Express* **28**, 33619 (2020).
24. H. Ito, Y. Kusunoki, J. Maeda, D. Akiyama, N. Kodama, H. Abe, R. Tetsuya, and T. Baba, *Optica* **7**, 47 (2020).
25. S. Iwamoto, Y. Ota, and Y. Arakawa, *Opt. Mater. Express* **11**, 319 (2021).
26. H. Kagami, T. Amemiya, S. Okada, N. Nishiyama, and X. Hu, *Opt. Express* **29**, 32755 (2021).
27. L. Chen, M. Lopez-Garcia, M. P. C. Taverne, X. Zheng, Y.-L. D. Ho, and J. Rarity, *Opt. Lett.* **42**, 1584 (2017).
28. X.-T. He, E.-T. Liang, J.-J. Yuan, H.-Y. Qiu, X.-D. Chen, F.-L. Zhao, and J.-W. Dong, *Nat. Commun.* **10**, 872 (2019).
29. T. Ozawa, H. M. Price, A. Amo, N. Goldman, M. Hafezi, L. Lu, M. C. Rechtsman, D. Schuster, J. Simon, O. Zilberberg, and I. Carusotto, *Rev. Mod. Phys.* **91**, 015006 (2019).
30. W. Liu, M. Hwang, Z. Ji, Y. Wang, G. Modi, and R. Agarwal, *Nano Lett.* **20**, 1329 (2020).
31. Z. Shao, H. Chen, S. Wang, X. Mao, Z. Yang, X. Hu, and R. Ma, *Nat. Nanotechnol.* **15**, 67 (2020).

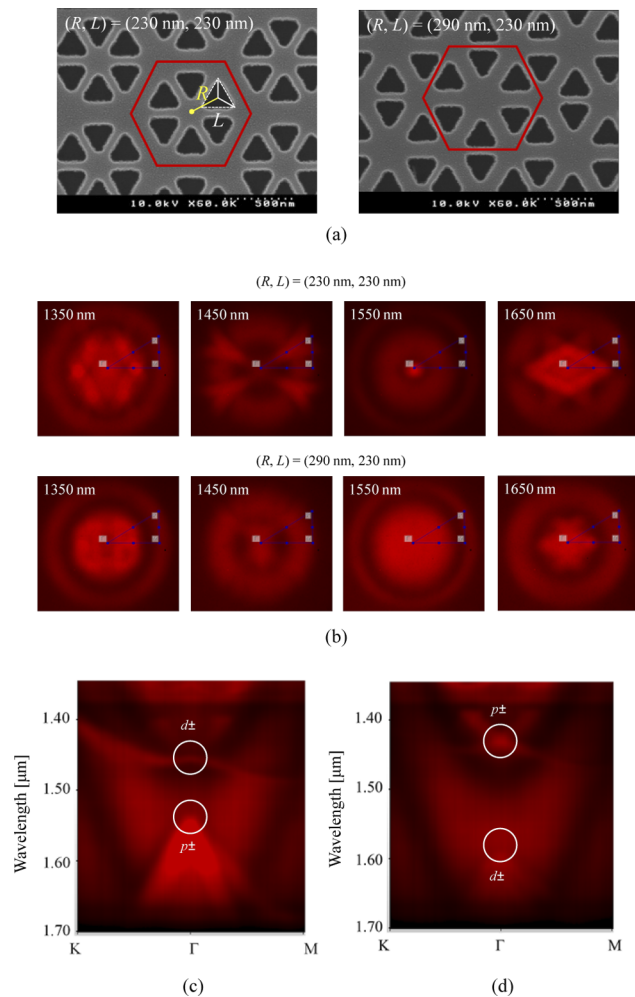


Fig. 4. (a) Scanning electron microscope image of topological photonic crystals used in the evaluation. (b) Fourier image of the scattered light from samples at a certain wavelength. (c), (d) Reconstructed band structures of photonic crystals distinct in topology, which was derived from the intensity along the Γ -K-M path in measured Fourier images.